

# Across the Arctic front west of Spitsbergen: high-resolution CTD sections from 1998–2000



Tuomo M. Saloranta & Harald Svendsen

The structure of the oceanic Arctic front west of Spitsbergen is investigated using data from high-resolution CTD sections from September 1998–2000. Below the fresher surface layer, the front appears as a temperature–salinity front situated near the shelf break. No clear corresponding front in density is found. Our analysis suggests that barotropic front instability is a main factor in provoking subsurface cross-front exchange. The subsurface heat loss in the West Spitsbergen Current due to this exchange is estimated to be of the same order of magnitude as the heat loss to the atmosphere in the surface layer.

*T. M. Saloranta, Dept. of Geophysics, University of Oslo, Box 1022 Blindern, N-0315 Oslo, Norway; H. Svendsen, Geophysical Institute, University of Bergen, Allégaten 70, N-5007 Bergen, Norway.*

The oceanic Arctic front west of Spitsbergen marks the boundary between two different water masses: the warm Atlantic type water (AW) in the West Spitsbergen Current (WSC) flowing along the continental slope, and the Arctic type colder and fresher water (ARW) onshore on the continental shelf (Fig. 1). While numerous studies on the WSC have been published (see, e.g. Gascard et al. 1995; Saloranta 2001), the properties and origin of the shelf waters are less documented. Presumably, ARW (and, seasonally, sea ice) is transported by the East Spitsbergen Current, possibly joining with an extension of the Bear Island Current, from Storfjorden to the Spitsbergen shelf where a mean northward flow prevails (Johannessen 1986; Loeng 1991; Saloranta 2001) (Fig. 1). The glaciers and rivers on the Spitsbergen coast, especially within fiords, are additional freshwater sources.

The Arctic front west of Spitsbergen is part of the larger and more or less continuous Arctic front system in the Nordic seas. Its southward continuation is the Arctic front in the Barents Sea (Johannessen & Foster 1978; Loeng 1991; Gawarkiewicz & Plueddemann 1995; Parsons et al. 1996; Harris et al. 1998) and westward continuation the Arctic front in the Norwegian–Green-

land Sea, west of the WSC (Van Aken et al. 1995). Generally, the position of the fronts in the Nordic seas is well correlated with bathymetry due to topographic steering of the currents (Appendix A), and the drop in salinity across such a front is usually accompanied with a drop in temperature, which weakens the density gradient across the front (Johannessen 1986).

In contrast to, e.g. the Arctic front in the Barents Sea, relatively little attention has been given to the Arctic front west of Spitsbergen. However, water exchange across this front may effectively dispose heat from the WSC, especially (i) in the subsurface water column (i.e. below 50 - 100 m) where the vertical heat flux to atmosphere is much reduced, and (ii) in the warm core of the WSC, which is situated next to the front over the upper part of the continental slope (Boyd & D'Asaro 1994; Gascard et al. 1995; Haugan 1999a; Saloranta 2001) and which is an important transporter of heat into the Arctic Ocean (Aagaard et al. 1987; Bourke et al. 1988; Gascard et al. 1995; Manley 1995; Haugan 1999b; Saloranta & Haugan 2001). Locally, the varying influence of the AW on the shelf and in the fiords can affect the composition and distribution of ecosystems therein (e.g. benthos [Blacker 1957]) as well as

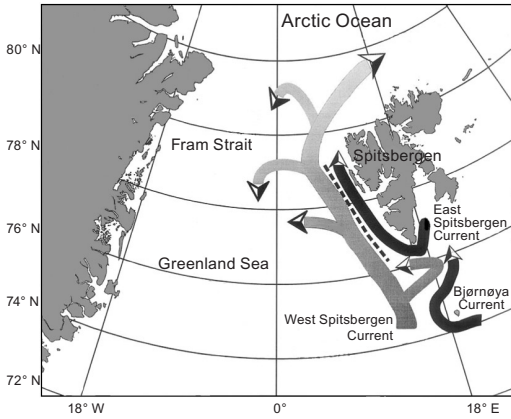


Fig. 1. Schematic illustration of the current patterns in the sea west of Svalbard, based on Johannessen (1986), Loeng (1991) and Gascard et al. (1995). Grey shaded arrows denote warm currents of Atlantic origin and black arrows colder currents of Arctic origin. Dashed line denotes the Arctic front west of Spitsbergen.

the local sea ice conditions decisive for the access of marine traffic to the communities on Spitsbergen in the winter months.

In this study, the structure of the Arctic front west of Spitsbergen is investigated using data from high-resolution CTD sections crossing the front.

## Background

On the basis of topographic steering of currents (Appendix A) and of knowledge of the WSC and slope–shelf systems in general we can anticipate the following main features in the slope–shelf system west of Spitsbergen.

(1) The warm AW core of the WSC (hereafter referred to as AW core) is, as already pointed out, confined over the upper continental slope where the maximum mean current speed has also been observed (Fahrback et al. 2001). In addition, an onshore thickening wedge of fresher surface waters over the shelf (and partly over the slope) was revealed in the mean hydrographic cross-slope structure presented by Saloranta (2001).

(2) The Arctic front resides near the shelf break between (i) the AW in the swift WSC, which is topographically well steered along the rather smooth isobaths of the steep slope (Hanzlick 1983; Jónsson et al. 1992; Poulain et al. 1996; Woodgate et al. 1998), and (ii) the ARW on the

relatively flat shelf, where the bottom topography is more irregular and characterized by banks and valleys (Fig. 2). Owing to the ragged shelf bottom topography, the mean flow is probably weaker on the shelf than over the slope (Boyd & D’Asaro 1994), consisting of more variable and rather closed circulation cells (see Sætre 1999). As the shelf break is generally found around 300 m depth, the front would be confined to the about 0–300 m layer. Moreover, Condie (1993) showed theoretically that a density front will tend to intersect the bottom close to the shelf break. Studies of the Arctic front in the Barents Sea (Johannessen & Foster 1978; Gawarkiewicz & Plueddemann 1995; Parsons et al. 1996; Harris et al. 1998) have indicated that the front there is indeed well correlated with bathymetry, moving about  $\pm 5$  km back and forth at the surface due to tides. As the slope west of Spitsbergen is much steeper than the slope in these studies, even stronger topographic steering can be anticipated in our case.

(3) While topographic steering of currents may inhibit cross-front exchange, there are numerous mechanisms that can act the other way (Huthnance 1995; Brink 1998). For example, baroclinic and barotropic instability, wind forcing in the surface layer as well as the many submarine valleys and other topographic irregularities on the shelf likely affect the current patterns, provoke front instability (meandering, vortices) and enhance cross-front exchange via ageostrophic effects (friction, nonlinearities, small spatio-temporal scales) relaxing the conditions required for topographic steering (Appendix A) (Huthnance 1995; Brink 1998).

Moreover, since the current speed and net volume transport are likely much larger in the WSC than on the shelf, it would be more likely to find remnants of the slope water (i.e. AW) on the shelf than remnants of the shelf water over the slope. While the role of the shelf waters in the WSC cooling is still rather uncertain, the relatively light ice conditions in the Spitsbergen fiords lacking a shallow sill (undocumented, but familiar to individuals with local experience) qualitatively suggest that the contribution of the AW to the oceanic heat flux therein is significant.

## Data and methods

During the three cruises of R/V *Håkon Mosby* in 1998–2000, each year in September, several

CTD sections were conducted across the slope and the shelf using a towed undulating SeaSoar CTD instrument (see Orvik et al. 1995). This data reveals the hydrographic structure within the 0 - 250 m layer with a horizontal resolution of 1 - 3 km. Five of these sections (S1–S5) are presented here (Fig. 2, Table 1). The total length of these sections is about 500 km.

The data is post-processed and pressure averaged to depth intervals of 2 m. As no rigorous calibration against water samples was done, the accuracy of the SeaSoar CTD is not exactly known. However, since we are focussing on changes in temperature and salinity rather than on the absolute values, the precision (random error) of the SeaSoar CTD is more relevant in our context. It is  $\pm 0.005$  °C and  $\pm 0.005$  mS ( $\approx \pm 0.006$  psu), which is more than adequate for our purpose.

The 34.9 psu isohaline is used here to roughly demarcate the more saline AW from the fresher ARW (Swift & Aagaard 1981; Manley 1995). The 300 m isobath (Fig. 2) is chosen to mark the shelf break (hereafter referred to as SB).

## Results

We first present the temperature–salinity (TS) structures of the five CTD sections (Figs. 2, 3) and then outline some qualitative features of the corresponding density structures (Fig. 4). In the following we speak in terms of 25 m depth intervals (0, 25, 50 m,...).

In 1998, the southern subsection of S1 reveals the AW core over the upper slope, i.e. between about 300 - 1000 m isobaths. The corresponding TS front, below the 0 - 25 m layer, is scarcely resolved at the beginning of the section on the quite narrow and steep part of the shelf. In the northern subsection of S1, the AW core is abruptly

terminated below 75 m depth near (slightly offshore) the SB, where a strong vertical TS front is observed (note that the slope is steeper here than in the southern subsection, possibly causing the AW core to contract horizontally due to topographic steering). Remnants of AW are found onshore of the TS front, and above it, a tongue of AW stretches onshore around 50 m depth under a fresher and strongly stratified surface layer extending over the upper slope. The hydrographic structure is very uniform in the 35 km long along-slope subsection which links the southern and northern subsections.

In 1999, in S2 the AW core extends onto the shelf about 20 km onshore of the SB. The corresponding front is most distinct in salinity, but is associated with a temperature front below about 50 m depth. A small slightly colder and fresher intrusion is seen about 10 km offshore of the SB.

Section S3 repeats partly the track of S1 taken one year earlier. Although the AW core in S3 is more extensive than in S1, the TS maxima lie similarly over the upper slope and the AW core is fading offshore. A TS front is observed near (slightly onshore) the SB in the 25 - 200 m layer, and some remnants of AW are seen onshore of this TS front, as in S1. Noteworthy is also the onshore thickening wedge of fresher surface water with subsurface temperature maximum.

In 2000, in S4 a TS front is again found near the SB below the fresher surface water wedge. On the shelf, extensive but somewhat “eroded” remnants of AW are observed. The last section, S5, runs over the tracks of S1 and S3. Also this section reveals extensive AW remnants near and onshore of the SB, below a fresher surface water wedge. Especially noteworthy is the AW column over the SB, which seems to be detaching from the rather uniform AW core, as it is already separated from this core by a narrow vertical column of ARW.

The density structures of S1–S5 (Fig. 4) reveal

*Table 1.* Information on the sections S1–S5. The column “Tide at the SB” gives the phase of the semidiurnal tide at the time when the section is crossing the shelf break (L denotes low water and H high water). Values correspond to tide at Longyearbyen (S2 and S4) and Ny-Ålesund (S1, S3 and S5), Svalbard. The column “Wind” gives the average wind speed and direction during the section, as measured by the weather station on R/V *Håkon Mosby*.

Section	Date	Starting at	Ending at	Duration	Tide at the SB	Wind
S1	6–7 Sept. 1998	78.7° N, 9.9° E	79.0° N, 10.7° E	15.5 h	1 h and ½ h after L	8 m s <sup>-1</sup> , 310°
S2	7–8 Sept. 1999	77.6° N, 9.8° E	77.7° N, 12.1° E	4.5 h	1 h after H	13 m s <sup>-1</sup> , 95°
S3	14 Sept. 1999	79.0° N, 6.7° E	79.0° N, 11.4° E	7 h	½ h after L	10 m s <sup>-1</sup> , 165°
S4	7–8 Sept. 2000	77.7° N, 14.2° E	77.2° N, 10.9° E	7.5 h	3 h after L	7 m s <sup>-1</sup> , 120°
S5	9 Sept. 2000	79.1° N, 7.7° E	79.0° N, 11.1° E	5.5 h	3 h after L	6 m s <sup>-1</sup> , 65°

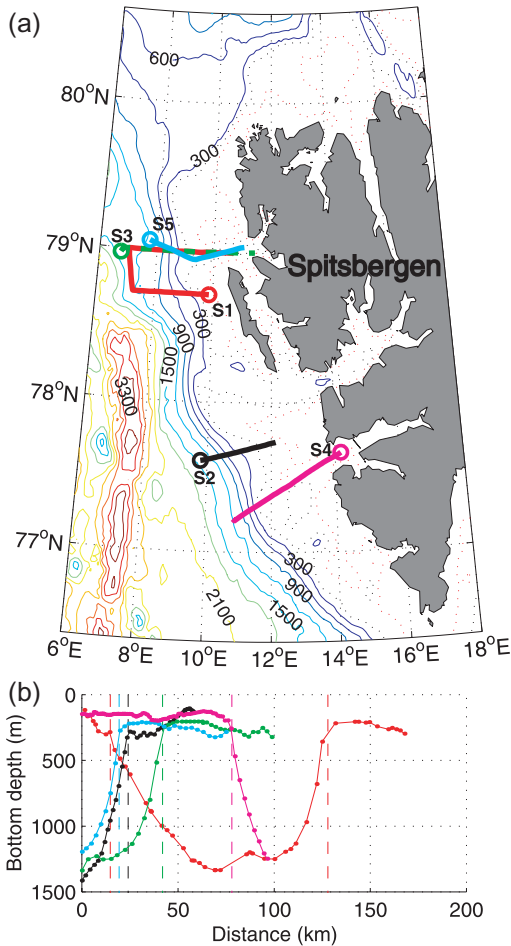


Fig. 2. (a) The location of the SeaSoar CTD sections: S1 (red), S2 (black), S3 (green, dashed line), S4 (magenta) and S5 (blue). Circles denote section starting points. Bottom topography is based on Jakobsson et al. (2000); solid contours show isobaths of 300, 600, 900 m..., and dotted contours 100 m (red) and 200 m (black) isobaths. (b) The bottom depth profiles of the CTD sections, based on the sonar measurements on R/V *Håkon Mosby*. Vertical dashed lines denote the corresponding position of the 300 m isobath (i.e. the shelf break).

generally no clear subsurface density fronts associated with the TS fronts, but isopycnals connect the AW and ARW across the TS front. A stronger subsurface horizontal density gradient is rather seen on the offshore side of the AW core, which is associated with a trough of lighter water (this feature is resolved by S1 and S3, and was also revealed in the mean hydrographic cross-slope structure presented by Saloranta [2001]).

A density front is, however, found in the surface layer (Fig. 4). This front is associated with the

fresher shelf waters often appearing as a wedge. This wedge extends variably also over the upper slope capping parts of the AW core (especially in S1).

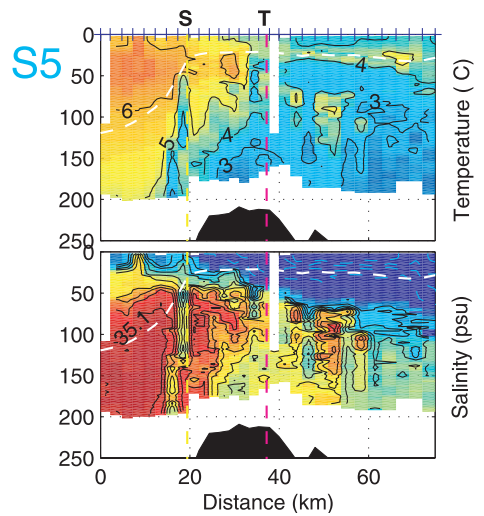
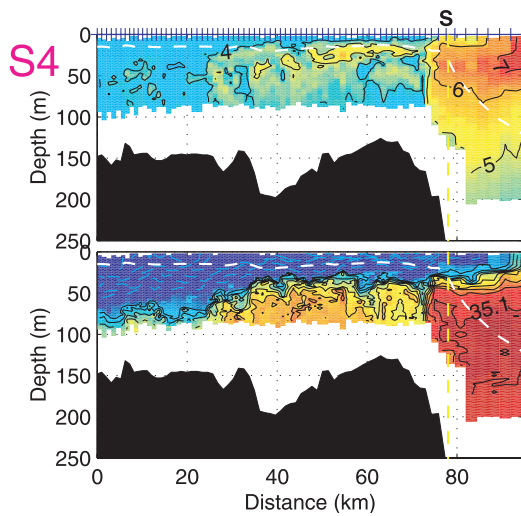
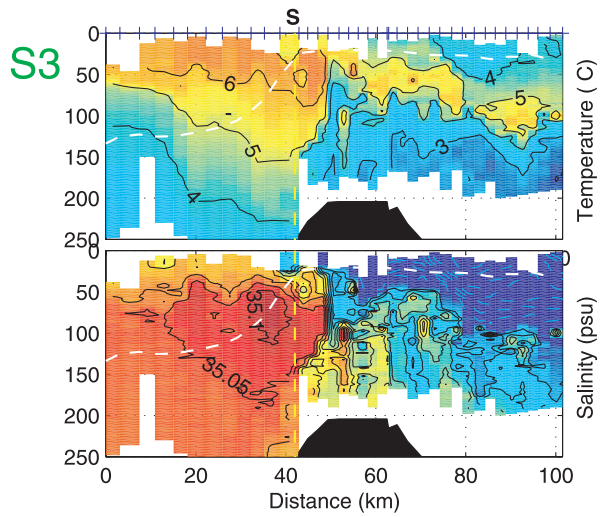
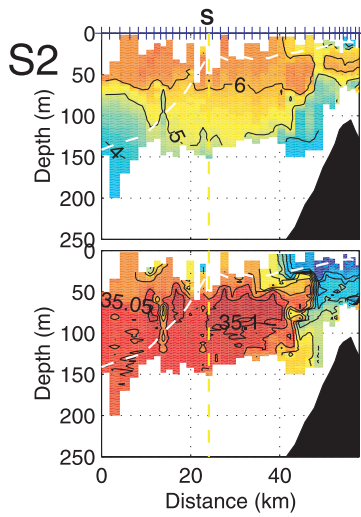
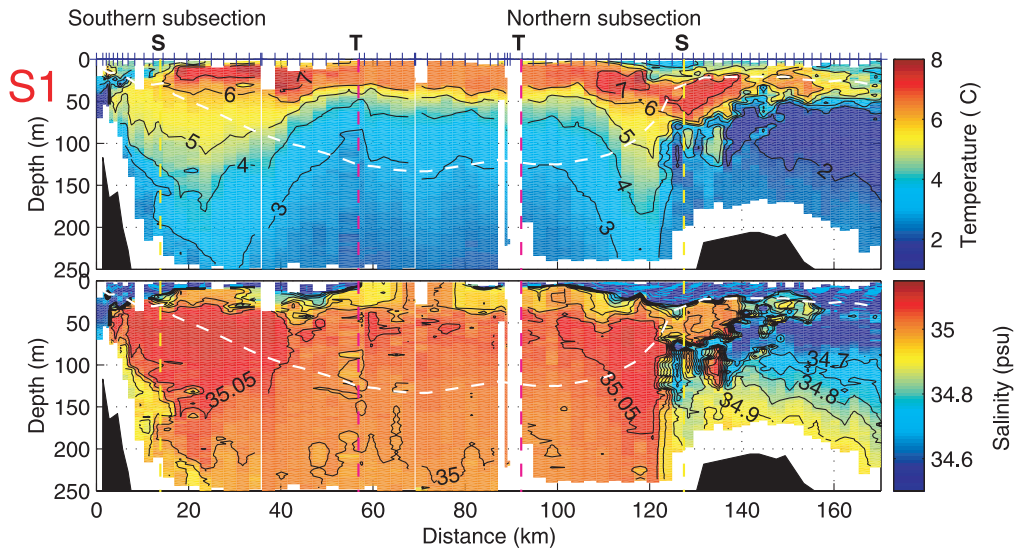
## Discussion

The Arctic front west of Spitsbergen can seemingly be divided into two, surface and subsurface fronts. The subsurface front, which will be our main focus here, is a TS front between the AW core and the shelf waters, where due to the balancing TS changes no clear density front is formed. As anticipated in the Background section, above, it is often capped by a shallow (0 - 50 m) and usually onshore thickening layer of fresher waters in which the surface front, rather strong in density, is found. The salinity stratified surface layer is influenced by surface phenomena, such as freshwater supply from glaciers and rivers (especially via the major fiords of Spitsbergen), wind forcing, heat exchange with atmosphere and solar heating, which explains the large variability in its TS properties and in the surface front position.

Many of the observed features of the subsurface front also agree with the expectations outlined earlier. For example, the AW core is observed over the upper slope and the Arctic front is most often found near the SB. The subsurface front seems to extend down to near the bottom, although the temperature contrast in particular fades somewhat with depth due to cooler AW at deeper levels.

In S2, the subsurface front and the AW core extend anomalously far onshore over the shelf, deviating somewhat from what we anticipated above. This might, however, be a *reversible* situation, a temporary deviation not contributing to net cross-front exchange. Other sections show rem-

Fig. 3 (right). Temperature and salinity in sections S1–S5. Contours (black solid lines) are drawn for values  $\geq 2^\circ\text{C}$  and  $\geq 34.7$  psu at  $1^\circ\text{C}$  and  $0.05$  psu intervals. Values lower than that are indicated by light blue dashed contours at  $2^\circ\text{C}$  and  $0.3$  psu intervals. The colour bars in the upper right corner apply to all sections; the darkest blue colour indicates values  $\leq 1^\circ\text{C}$  and  $\leq 34.5$  psu. Black areas mark the bottom (based on sonar measurements on R/V *Håkon Mosby*), and white dashed line similarly bottom depth in decameters (10 m) according to the scale on the y-axis. Yellow vertical dashed line marked with “S” denotes the position of the 300 m isobath (i.e. shelf break; see Fig. 2), and magenta vertical dashed line marked with “T” a turning point in the section track. Ticks at the surface denote “stations”, i.e. downward dives of the SeaSoar CTD.



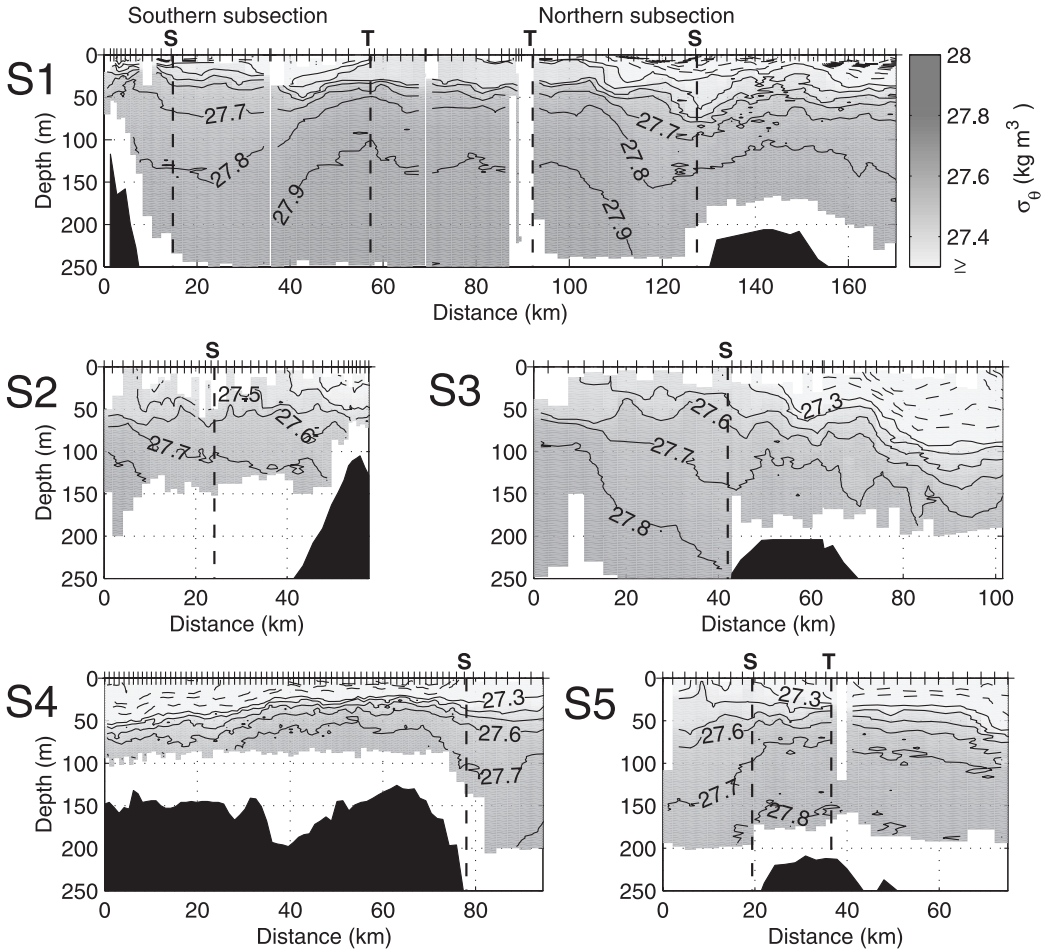


Fig. 4. Potential density ( $\sigma_\theta$ ) of sections S1–S5. The colour bar in the upper right corner applies to all sections. Solid contours are drawn for values  $\geq 27.3 \text{ kg m}^{-3}$  at  $0.1 \text{ kg m}^{-3}$  intervals. Values lower than that are indicated by dashed contours at  $0.3 \text{ kg m}^{-3}$  intervals and by the lightest shading. Vertical dashed lines marked with “S” and “T” denote the position of the 300 m isobath (i.e. shelf break; see Fig. 2) and a turning point in the section track, respectively. Ticks at the surface denote “stations”, i.e. downward dives of the SeaSoar CTD.

nants of AW on the shelf, which is indicative of *irreversible* cross-front exchange. In S4 the AW remnants seem to be relatively old, since their properties have faded, while in S5 a possibly new detaching remnant can be seen. Moreover, as anticipated above, AW remnants are more usually observed on the shelf than ARW remnants over the slope.

As pointed out, many different mechanisms could cause such irreversible cross-front exchange. As there is no clear subsurface density front associated with the TS front, we can, however, as a “first order” approximation neglect processes

connected to density fronts, such as baroclinic front adjustment and baroclinic instability.

Some of the AW “leaking” onto the shelf could be associated with the submarine valleys cutting across the shelf and deviating the topographically steered AW flow from the slope onto the shelf. The northern subsection of S1, as well as S3 and S5, run over such a valley (Kongsfjordrenna), but only S5 reveals more extensive remnants of AW. The onshore deviating AW core in S2 might be connected to the about 300 m deep “niche” onshore of the SB (see bottom profiles in Figs. 2, 3). AW remnants are, however, also found over

a bank in S4. Therefore, while these valleys may assist leaking, the AW remnants are seemingly not only confined to them.

Tidal currents (max.  $0.1 - 0.3 \text{ m s}^{-1}$  according to Kowalik & Proshutinsky [1994]) are expected to cause only minor horizontal deviations of a few kilometres at maximum, e.g. in the front position. No clear coherence between the tidal phase (Table 1) and the subsurface front position can be detected in our sections.

Coastal upwelling might sporadically bring AW onto the shelf. If the leaking seen in S2 was provoked by upwelling, we would expect to see also extensive capping of the AW core by the fresher surface layer. This is however not the case. The wind speeds (Table 1) measured during the acquisition of the sections were generally low. Moreover, the wind direction during S2 was easterly (the prevailing wind direction), which does not favour upwelling either.

The structure of the few ARW intrusions in our observations was rather vertically elongated, contrary to the thin lens-like intrusions observed by Haugan (1999a). Similar vertical shape characterized also parts of the subsurface Arctic front. This would agree with the hypothesis that barotropic instability, arising from the velocity shear between the rather unidirectional and barotropic WSC (Fahrbach et al. 2001) and presumably weaker but more complicated flow on the shelf, is an important source of frontal mixing generating waves and vortex fields near the SB and hence shedding remnants of AW onto the shelf and vice versa.

Although we cannot derive cross-front exchange rates from our hydrographic data only, we can give a rough order-of-magnitude estimate for the heat loss from the warm core of the WSC due to cross-front exchange. We first assume that the irreversible shelf-slope exchange is generally of order: slope current transport per 1000 km along the slope (Huthnance 1995). A typical subsurface temperature difference of about  $2 \text{ }^{\circ}\text{C}$  (Fig. 3) between the slope (AW core) and the shelf waters would then indicate a slope current cooling of  $0.2 \text{ }^{\circ}\text{C}/100 \text{ km}$  along the slope due to cross-front exchange. This value corresponds well to the observed mean along-slope cooling of the WSC below 50 m,  $0.2 - 0.4 \text{ }^{\circ}\text{C}/\text{latitude}$  (Saloranta 2001). The cooling of  $0.2 \text{ }^{\circ}\text{C}/100 \text{ km}$  in, e.g. the 100 - 200 m layer would correspond to a mean vertical heat flux of about  $100 \text{ W m}^{-2}$ , assuming a typical mean speed of  $0.15 \text{ m s}^{-1}$  for the part of

the WSC confined over the upper slope (Fahrbach et al. 2001). This subsurface heat loss is of the same magnitude as the mean surface heat loss to the atmosphere for the autumn season (Häkkinen & Cavalieri 1989), acting on, e.g. the 0 - 100 m layer.

## Conclusions

In the surface layer, the Arctic front appears as a density front associated with fresher surface waters (usually appearing as an onshore thickening wedge). Below this 0 - 50 m surface layer, the Arctic front appears only as a TS front and a corresponding density front is missing. This subsurface Arctic TS front seems to be confined near the shelf break and extends down near to the bottom. AW remnants found on the shelf provide evidence for significant irreversible cross-front exchange. The missing density front as well as the vertical shape in the TS front structures suggest that barotropic front instability is a main cause for subsurface cross-front exchange. The heat loss in the WSC due to this exchange can apparently be of the same order of magnitude as the surface heat loss to the atmosphere.

*Acknowledgements.*—We owe grateful thanks to captain Ole Magnus Røttingen and his crew, Peter Haugan, Tor Gammelsrød, scientific engineers, as well as students onboard the 1998–2000 cruises of R/V *Håkon Mosby*. Thanks also to those involved in the post-processing of the data and to the two anonymous reviewers. This study is a part of the research programme “Arktisk lys og varme”, funded by the Research Council of Norway.

## Appendix A

The topographic steering of currents arises from the conservation of potential vorticity. On the basis of the momentum and continuity equations, and when assuming no friction, hydrostatic conditions and homogeneous fluid, it can be shown that:

$$\frac{DQ}{Dt} = 0, \quad Q = \frac{f + \zeta}{H + \eta}, \quad \zeta = \frac{\partial v}{\partial x} - \frac{\partial u}{\partial y}, \quad (1)$$

where  $Q$  is potential vorticity,  $f$  is coriolis parameter (planetary vorticity),  $\zeta$  is relative vor-

ticity,  $H$  is the depth of the water column,  $\eta$  is surface elevation, and  $u$  and  $v$  are the horizontal velocity components ( $\hat{u} = u\hat{i} + v\hat{j}$ ). Assuming stationary conditions,  $|\zeta| \ll f$ ,  $|\eta| \ll H$ , and in addition  $|\nabla\zeta| \ll |\nabla\eta|$  and  $|\nabla\eta| \ll |\nabla H|$ , we get:

$$\hat{u} \cdot \nabla \left( \frac{f}{H} \right) = 0, \quad (2)$$

which tells us that on an  $f$ -plane (constant  $f$ ) the current will follow contours of constant bottom depth, i.e. isobaths. (For details see, e.g. Gill 1982.)

## References

- Aagaard, K., Foldvik, A. & Hillman, S. R. 1987: The West Spitsbergen Current: disposition and water mass transformation. *J. Geophys. Res.* 92(C4), 3778–3784.
- Blacker, R. W. 1957: *Benthic animals as indicators for hydrographic conditions and climatic change in Svalbard waters. Fishery Investigations, Series 2, 20(10)*. Ministry of Agriculture, Fisheries and Food. London: Her Majesty's Stationary Office.
- Bourke, R. H., Weigel, A. M. & Paquette, R. G. 1988: The westward turning branch of the West Spitsbergen Current. *J. Geophys. Res.* 93(C11), 14065–14077.
- Boyd, T. J. & D'Asaro, E. A. 1994: Cooling of the West Spitsbergen Current: wintertime observations west of Svalbard. *J. Geophys. Res.* 99(C11), 22597–22618.
- Brink, K. H. 1998: Deep-sea forcing and exchange processes. In K. H. Brink & A. R. Robinson (eds.): *The sea. Vol. 10*. Pp. 151–167. New York: John Wiley & Sons.
- Condie, S. A. 1993: Formation and stability of shelf break fronts. *J. Geophys. Res.* 98(C7), 12405–12416.
- Fahrbach, E., Meincke, J., Østerhus, S., Rohardt, G., Schauer, U., Tverberg, V. & Verduin, J. 2001: Direct measurements of volume transports through Fram Strait. *Polar Res.* 20, 217–224 (this issue).
- Gascard, J.-C., Richez, C. & Rouault, C. 1995: New insights on large scale oceanography in Fram Strait: the West Spitsbergen Current. In W. O. Smith & J. M. Grebmeier (eds.): *Arctic oceanography: marginal ice zones and continental shelves. Coastal and Estuarine Studies 49*. Pp. 131–182. Washington D.C.: American Geophysical Union.
- Gawarkiewicz, G. & Plueddemann, A. J. 1995: Topographic control of thermohaline frontal structure in the Barents Sea polar front on the south flank of Spitsbergen Bank. *J. Geophys. Res.* 100(C3), 4509–4524.
- Gill, A. E. 1982: *Atmosphere–ocean dynamics*. London: Academic Press.
- Häkkinen, S. & Cavalieri, D. J. 1989: A study of oceanic surface heat fluxes in the Greenland, Norwegian and Barents seas. *J. Geophys. Res.* 94(C5), 6145–6157.
- Hanzlick, D. J. 1983: *The West Spitsbergen Current: transport, forcing and variability*. PhD thesis, University of Washington.
- Harris, C. L., Plueddemann, A. J. & Gawarkiewicz, G. 1998: Water mass distribution and polar front structure in the western Barents Sea. *J. Geophys. Res.* 103(C2), 2905–2917.
- Haugan, P. M. 1999a: Structure and heat content of the West Spitsbergen Current. *Polar Res.* 18, 183–188.
- Haugan, P. M. 1999b: *On transports of mass, heat and carbon in the Arctic Mediterranean*. PhD thesis, University of Bergen.
- Huthnance, J. M. 1995: Circulation, exchange and water masses at the ocean margin: the role of physical processes at the shelf edge. *Prog. Oceanogr.* 35, 353–431.
- Jakobsson, M., Cherkis, N. Z., Woodward, J., Macnab, R. & Coakley B. 2000: New grid of Arctic bathymetry aids scientists and mapmakers. *Eos Trans.* 81, 89–96.
- Johannessen, O. M. 1986: Brief overview of the physical oceanography. In B. G. Hurdle (ed.): *Nordic seas*. Pp. 103–127. New York: Springer.
- Johannessen, O. M. & Foster, L. A. 1978: A note on the topographically controlled oceanic polar front in the Barents Sea. *J. Geophys. Res.* 83(C9), 4567–4571.
- Jónsson, S., Foldvik, A. & Aagaard, K. 1992: The structure and atmospheric forcing of the mesoscale velocity field in Fram Strait. *J. Geophys. Res.* 97(C8), 12585–12600.
- Kowalik, Z. & Proshutinsky, A. Y. 1994: The Arctic Ocean tides. In O. M. Johannessen et al. (eds): *Polar oceans and their role in shaping the global environment. Geophysical Monograph 85*. Pp. 137–158. Washington D.C.: American Geophysical Union.
- Loeng, H. 1991: Features of the physical oceanographic conditions of the Barents Sea. *Polar Res.* 10, 5–18.
- Manley, T. O. 1995: Branching of Atlantic water within the Greenland–Spitsbergen passage: an estimate of recirculation. *J. Geophys. Res.* 100(C10), 20627–20634.
- Orvik, K. A., Lundberg, L. & Mork, M. 1995: Topographic influence on the flow field off Lofoten–Vesterålen. In H. R. Skjoldal et al. (eds.): *Ecology of fjords and coastal waters*. Pp. 165–175. Amsterdam: Elsevier Science.
- Parsons, A. R., Bourke, R. H., Muench, R. D., Chiu, C.-S., Lynch, J. F., Miller, J. H., Plueddemann, A. J. & Pawlowicz, R. 1996: The Barents Sea polar front in summer. *J. Geophys. Res.* 101(C6), 14201–14221.
- Poulain, P.-M., Warn-Varnas, A. & Niiler, P. P. 1996: Near-surface circulation of the Nordic seas as measured by Lagrangian drifters. *J. Geophys. Res.* 101(C8), 18237–18258.
- Saloranta, T. M. 2001: *Hydrographic structure of the sea west of Svalbard along and across the continental slope. Reports in Meteorology and Oceanography 2*. University of Bergen.
- Saloranta, T. M. & Haugan, P. M. 2001: Interannual variability in the hydrography of Atlantic water northwest of Svalbard. *J. Geophys. Res.* 106(C7), 13931–13943.
- Swift, J. H. & Aagaard, K. 1981: Seasonal transitions and water mass formation in the Iceland and Greenland seas. *Deep-Sea Res.* 28A, 1107–1129.
- Setre, R. 1999: Features of the central Norwegian shelf circulation. *Cont. Shelf Res.* 19, 1809–1831.
- Van Aken, H. M., Budeus, G. & Hähnel, M. 1995: The anatomy of the Arctic Frontal Zone in the Greenland Sea. *J. Geophys. Res.* 100(C8), 15999–16014.
- Woodgate, R. A., Schauer, U. & Fahrbach, E. 1998: *Moored current meters in the Fram Strait at 79° N: preliminary results with special emphasis on the West Spitsbergen Current. Ber. Fachber. Phys. 91*. Bremerhaven: Alfred Wegener Institute for Polar and Marine Research.